RSC Advances

ROYAL SOCIETY OF CHEMISTRY

www.rsc.org/advances

Graphical Abstract:

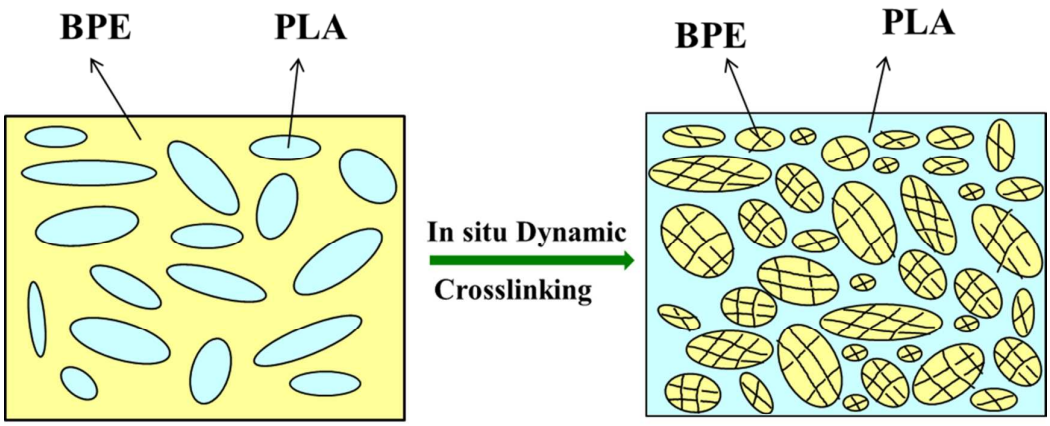

Novel biobased thermoplastic elastomer consisting of synthetic polyester elastomer and polylactide by in situ dynamical crosslinking method

Hailan Kang,[a,c] *Xiaoran Hu,*[a,b] *Manqiang Li*[a,b] *Liqun Zhang,*[*,a,b] *Youping Wu,*[a,b] *Nanying Ning,*[a,b] *Ming Tian*[a,b]

[a]State Key Laboratory of Organic-Inorganic Composites, Beijing University of Chemical Technology, Beijing 100029, P. R. China

[b]Key Laboratory of Beijing City for Preparation and Processing of Novel Polymer Materials, Beijing University of Chemical Technology, Beijing 100029, P. R. China

[c]College of Materials Science and Engineering, Shenyang University of Chemical Technology, Shenyang, 110142, China

CORRESPONDING AUTHOR FOOTNOTE: Correspondences should be addressed to Prof L. Q. Zhang at ZhangLQ@mail.buct.edu.cn.

ABSTRACT: Owing to the sustainability and environmental friendliness of biobased polymers, we adopted synthesized biobased polyester elastomer (BPE) and polylactide (PLA) as the two components to produce a new biobased thermoplastic vulcanizate (TPV) by an in situ dynamical crosslinking and mixing method. The effects of blending ratio on the dynamic crosslinking and micromorphology of TPV were investigated by mixing torque measurements, degree of crosslinking measurements, TEM, DSC, and rheological properties. A large amount of crosslinked BPE particles were dispersed in the PLA continuous phase, with the particle sizes ranging from 1 to 4 μm, indicating the occurrence of phase inversion during the dynamical crosslinking and mixing process. The tensile strength and elongation at break of the biobased TPVs ranged from 11.4 MPa to 17.8 MPa and 154% to 184%, respectively. Reprocessing did not significantly reduce the mechanical properties, as an indication that biobased TPVs, like thermoplastics, have good reprocessability. In vitro cytotoxicity tests showed that our TPVs were nontoxic, at least towards mouse fibroblasts. Thus, these novel biobased TPVs with excellent mechanical properties and low cytotoxicity are reported for the first time in the flied of thermoplastic elastomers for engineering and biomedical applications.

KEYWORDS: Biobased thermoplastic vulcanizate; Morphology; Reprocessability; Biocompatibility

INTRODUCTION

Thermoplastic elastomers (TPEs) behave like conventional elastomers, but they are thermoplastic and can be reshaped and recycled. TPEs represent a great technological advance since they pose less threat to the environment.[1] Compared with traditional rubbers, TPEs do not require further crosslinking, can be processed in simple machines, and consume less energy. Besides, the scraps generated during production can be reground and recycled, which could save the petroleum resources and reduce environmental pollution. TPEs have proven themselves in meeting a wide range of demanding engineering requirements in automotive applications.[2]

TPEs are classified into two categories according to the method of preparation: (i) chemically synthesized TPEs, including styrenic block copolymers, thermoplastic copolyesters, thermoplastic polyurethanes, and thermoplastic polyamides; (ii) blends and elastomeric alloys, containing elastomer-plastic simple blends, thermoplastic vulcanizates (TPVs), and melt-processable rubbers.[3] TPVs are a very special class of TPEs, consisting of a thermoplastic matrix and a crosslinked elastomer as the dispersed phase.[3-5] TPVs are produced by dynamic crosslinking, which consist of the selective crosslinking of the vast elastomer and its fine dispersion in the thermoplastic under intensive mixing. The elastomer is the majority component, and its weight fraction is greater than 50%. The increasing viscosity and elasticity of the elastomer through vulcanization affects the phase continuity and promotes the phase inversion, i.e. the majority phase becomes the dispersed phase.[6] TPVs have several advantages over the traditional thermoset elastomer. Functional properties of TPVs similar to those of thermoset elastomers can be obtained by using the classical processing tools for polymer melts, but, at the same time, TPVs are recyclable

as thermoplastics. TPVs have been widely applied to various fields such as the automobile, building, and electronic industries. Nowadays, TPV is produced worldwide at a rate of 450,000 tons per annum. Nevertheless, the current TPVs are blends of petroleum-dependent polymers such as ethylene–propylene–diene rubber (EPDM)/polypropylene (PP) blend, acrylonitrile–butadiene rubber (NBR)/PP blend, NBR/polyethylene (PE) blend, EPDM/PE blend, EPDM/nylon-6 blend, acrylate rubber (ACM)/nylon-6 blend, and butyl rubber (IIR)/polyamide blend.[7-13]

Biobased polymers have attracted much attention in the past decades owing to environmental concerns, climate change, and the depletion of fossil fuels. Biobased polymers are currently sustainable alternatives to conventional petroleum-based polymers, and these polymers derived from renewable resources mainly include starch-based polymers, polylactide (PLA), polyhydroxyalkanoates (PHAs), cellulosic-based polymers and soy-based polymers.[14-18] One of the most promising polymers in this regard is PLA, whose monomer has been produced by the microbial fermentation of agricultural by-products on a commercial scale.[19] PLA is not only renewable but also biodegradable; therefore, it has been used in medical materials, disposable plastics, and fibers. Although many biobased elastomers have been reported, such as poly(glycerol sebacate)[20], poly(polyol sebacate)[21], and poly(diol citrate)[22], these elastomers were designed for biomedical materials with fast degradation. Recently, our group has focused on the use of large-scaled biobased monomers to synthesize biobased elastomers with excellent mechanical properties and environment stability for engineering applications.[23-25]

The synthesis of TPEs based on renewable resources has also gained extensive academic interests. For example, biobased TPUs were synthesized from diphenylmethane diisocyanate, 1,4-butanediol,

and a polyol based on a di-functional dimer fatty acid.[26] Kobayashi et al. prepared novel biobased TPEs by the enzymatic copolymerization of macrolide as the hard segments and 12-hydroxystearate as the soft segments.[27] Wanamaker et al. developed a series of biobased TPEs with polylactide as the hard segments and polymenthide as the soft segments.[28] However, up to now, there is few report on using a blending method to prepare TPVs from biobased polymers. Consequently, the development of totally biobased TPVs is of great importance and highly desired in both academia and industry, providing an alternative to traditional petroleum-based TPVs.

Biobased polyester elastomer (BPE) synthesized from biobased diols and diacids have been developed in our laboratory.[23] These elastomers exhibit satisfactory elasticity, excellent mechanical properties after reinforcement and good biocompatibility. In the present work, biobased plastic (PLA) and biobased polyester elastomer (BPE) are chosen as the two components to prepare a new TPV derived exclusively from renewable resources by the dynamic in situ crosslinking method. The important reason for choosing PLA as the plastic matrix and BPE as the rubber matrix was the potential compatibility between PLA and BPE.[29] The effects of composition on the properties of the biobased TPVs, such as morphology, rheological properties, mechanical properties, reprocessability, and biocompatibility were studied. Biobased TPVs with both reprocessability and thermoplasticity were first reported by in situ dynamic crosslinking and mixing.

MATERIALS AND METHODS

Raw Materials. The polylactide (PLA) was purchased from Natureworks (USA) as grade 2002D. It has a density of 1.24 g/cm^3, a number-average molecular weight of ~133,000 g/mol, a polydispersity index of 1.50, a glass transition temperature of 60 ºC, and a melting point of 152 ºC. Our biobased polyester elastomer (BPE), which was synthesized according to a procedure described previously,[23, 29] had a number-average molecular weight of ~35,000 g/mol, a polydispersity index of 3.69, and a T_g of -56 ºC. The dicumyl peroxide (DCP) used was commercial product. The BPE chemical structures are shown in Scheme 1. BPE, with the presence of itaconate, can be readily crosslinked by dicumyl peroxide (DCP) into a network.

Preparation of Biobased TPVs. BPE and PLA were dried in a vacuum oven at 60 ºC for at least 12 h before processing. The dynamically crosslinked BPE/PLA blends were fabricated by the following steps: (i) a BPE/PLA premix was prepared by melt-mixing with a given blending ratio BPE/PLA (60/40, 70/30, or 80/20) for 5 min by using a Haake internal mixer (HAAKE Rheomix 600 OS, Thermal Fisher Scientific, USA) at 170 ºC at a rotational speed of 80 rpm; (ii) the BPE/PLA premix and DCP were mixed on a 6-inch two-roll mill at room temperature to produce a BPE/PLA blend; (iii) the BPE/PLA blend from step-(ii) was dynamically crosslinked for 8 min at 170 ºC at a rotational speed of 80 rpm in the Haake internal mixer. The dynamically crosslinked sample was hot-pressed at 180 ºC to form 1 mm thick sheets, which were then cold-pressed.

Characterization. The morphology was determined by an H-800-1 transmission electron microscope (Hitachi Co., Japan) at 200 kV. The samples were cryomicrotomed at -100 ºC to produce sections with 60 nm thickness, which were then vapor-stained with OsO_4 for 20 min.

The dumbbell-shaped specimens were measured according to ASTM D412 by using a CMT 4104 electrical tensile instrument (Shenzhen SANS Test Machine Co., Ltd., China) at a crosshead speed of 500 mm/min. For each BPE/PLA ratio, five specimens were tested and the average was taken. To evaluate the reprocessability of the biobased TPVs, we reprocessed each biobased TPV for five times by mixing the TPV in a Haake internal mixer for 8 min and compression molding at 180 ºC to form 1 mm thick sheets, and the tensile properties of the reprocessed biobased TPVs were measured. Rheological measurements were performed on an RPA 2000 rheometer (Alpha Technologies, Akron, Ohio). The strain scanning conditions were 180 °C, 1 Hz, and a strain range of 0.2-470%. For a detailed study on the performance of the reprocessed biobased TPVs, we reset the RPA strain scanning conditions to track the changes in rheological properties. Each sample underwent the following test sequences: (i) to simulate the mixing process, the following conditions were used: a temperature of 180 °C, a frequency of 1 Hz, and a strain range of 0.2-470%; (ii) to simulate the molding process, a temperature of 180 °C was maintained for 5 min. Each scanning process was repeated 5 times.

In vitro cytotoxicity testing was carried out on mouse fibroblasts (L-929) by MTT assays. All samples were sterilized with 75% ethanol and then rinsed twice with PBS solution. The samples were exposed to Co^{60} for 15 min and incubated in Dulbecco's modified Eagle's medium (DMEM) at a proportion of 3 cm^2/ml for 24 h at 37 ºC. The extract solution was then filtered (0.22 μm pore size) to eliminate any solid particles in the sample. L929 cells were grown in DMEM supplemented with 10% fetal bovine serum (FBS) at a density of 5.0×10^4 cells/well and incubated in 5% CO_2 under humidified conditions at 37 ºC. After the incubation, the medium was replaced by the

prepared extract dilution which was used as the new culture medium, while the initial medium was used as a negative control. The cells were allowed to proliferate for 3 days, and the number of viable cells was determined by adding 5 mg/mL of MTT in the culture medium. After a further incubation of 4 h, the medium was aspirated, the formed blue formazan crystals were dissolved in isopropanol (BDH, Poole, England), and the absorbance at 570 nm was determined. All sample extracts were tested at least three times to obtain consistent results. The relative viability was calculated by

$$Relative\ \ cell\ viability = (A_{test} - A_0)/(A_{control} - A_0) \quad (1)$$

where A_{test} is the absorbance of the sample, $A_{control}$ is the absorbance of the controlled well containing cells with DMEM, and A_0 is the absorbance of the solution containing only DMEM. The morphology of the sample incubated for 3 days was observed by an inverted phase contrast microscope before MTT testing.

RESULT AND DISCUSSION

Mixing Torque and Temperature. Figure 1 shows the mixing torque and temperature as a function of time during the dynamic crosslinking of the BPE/PLA blends with different blending ratios of BPE/PLA prepared by step-(ii) in section 2.2. Initially, the mixing torque increases with the increase in mixing time because of the introduction of the cold BPE/PLA blend into the mixer, and then decreases owing to the melting of the blend. The subsequent dramatic increase in mixing torque is related to the dramatic changes in the viscosity and elasticity of the BPE phase due to the crosslinking of BPE. After that, the torque slowly declines until the end of the dynamic crosslinking process, indicating the full homogenization of the biobased TPV. The temperature curve with different DCP contents exhibits a decrease with the introduction of the cold BPE/PLA blends into the hot mixer and the melting of the blends. Then the temperature increases continuously, surpassing the set temperature due to viscous energy dissipation and crosslinking. The stable torque and temperature of the biobased TPVs decrease as the BPE content increases because the high BPE content results in a lower viscosity of the whole system. Both the torque and temperature curves are similar to those reported for other dynamically crosslinked systems, such as EPDM/PP TPV[30, 31], NBR/PP TPV[9].

Morphology. TPV morphology, which is one of the most crucial characteristics, results from the complex relationship between the composition, viscosity, and elasticity ratios of the individual components, the processing conditions, and the crosslinking reaction. We firstly investigated the effect of crosslinking agent content on the morphology of the biobased TPVs. The TEM micrographs of the biobased TPVs with different DCP contents are depicted in Figure 2. In the

TEM micrographs, PLA appears as the light domains and BPE as the dark domains owing to the staining effect of the double bonds of BPE. PLA is dispersed in the BPE matrix and exhibits elongated structures for the BPE/PLA blend without DCP (Figure 2(a)), because BPE, in a larger amount than PLA, tends to form the continuous phase. With the addition of the curing agent DCP, BPE is dispersed in the PLA matrix; that is, phase inversion has occurred after the in situ dynamic crosslinking accompanied by mechanical mixing. The increase of DCP content increases the degree of crosslinking of BPE, which can be validated by the dynamic crosslinking curves (Figure S1) and extracting experiments (Figure S2) in the supporting information. For the biobased TPVs with a lower DCP content (0.02 phr) (Figure 2(b)), the crosslinked BPE in the shape of thin strips exhibits a larger particle size and heterogeneous distribution. A lower degree of crosslinking results in a smaller difference in viscosity between BPE and PLA and thus produces lower shear during the dynamical crosslinking process to separate the BPE particles. Besides, BPE flows and deforms more easily at a lower degree of crosslinking and is thus prone to aggregate, leading to its nonuniform dispersion in PLA matrix. The viscosity of the BPE phase increases with the increase of DCP content, resulting in an increase in the difference between the viscosities of BPE and PLA and an increase in the effective shear stress. The crosslinked BPE particles can be easily broken up into smaller particles during shear and dispersed homogeneously in the PLA matrix, as shown in Figure2(c). The higher the DCP content, the faster the crosslinking of the BPE phase and the earlier the occurrence of phase inversion. In a relatively short time, the curing rate becomes far greater than the shear rate, and it becomes too difficult for the PLA matrix, with a relatively low viscosity, to break up the highly crosslinked and very viscous BPE into small particles. Thus, a high degree of

crosslinking results in the aggregation of large particles, and the morphology is shown in Figures 2(d), 2(e). The particle size of BPE shown in Figure 2(c) is the smallest, demonstrating that the optimal DCP content is 0.06 phr. Therefore, in the latter investigations we adopted a DCP content of 0.06 phr to prepare biobased TPVs. The diagrams of phase inversion for biobased TPVs with different degree of crosslinking are shown in Scheme 2 to better illustrate the in situ dynamical crosslinking process.

The performance of TPV is also related to the blending ratio of elastomer to plastic. If the TPV contains high elastomer content, the performance of the TPV is close to that of traditional rubbers and TPV exhibits better elasticity than TPE. However, a higher elastomer content will lead to a higher difficulty in phase inversion and a larger size of the dispersion phase, thus resulting in a reduction in mechanical properties and a poor thermoplastic process ability. Thus, the effect of blending ratio on the morphology of biobased TPVs was investigated, and the TEM micrographs of biobased TPVs with different blending ratio are depicted in Figure 3. The morphology of TPV consists of vast BPE particles dispersed in the PLA continuous phase, indicating that the crosslinked BPE particles are broken up into small particles and the phase inversion takes place during the dynamic crosslinking process. The BPE particles have an irregular, oval or elongated shape. The particles size ranges from 1 to 4 μm, and some neighboring BPE particles are interconnected. At a high BPE content (Figure 3(c)), there is obvious aggregation in the BPE phase, resulting in a larger particle size and wide particle distribution. The high the BPE content, the higher the particle aggregation and the more difficult the breakup of crosslinked BPE particles. In other words, a higher BPE content makes phase inversion more difficult and results in larger BPE particles. These

results indicate that the blending ratio of elastomer to plastic has a great impact on the breakup of the crosslinked elastomer phase during dynamic crosslinking.

Thermal Properties. The thermal behavior of pure BPE, neat PLA, and biobased TPVs was investigated by DSC measurements. Figure 4 shows the DSC curves, and Table 1 summarizes the relevant data. All the biobased TPVs exhibit two clear glass transitions (T_g), demonstrating that BPE/PLA TPV is a phase-separated system during cooling. With the addition of BPE to PLA, the T_g of PLA shifts to lower temperatures, while the T_g of BPE shifts to higher temperatures. The shifts of these T_gs towards each other indicate some compatibility between PLA and BPE. The heat of cold crystallization (ΔH_{cc}) and the heat of melting (ΔH_m) for the BPE component of the biobased TPVs are lower than those for pure BPE because of the crosslinking of BPE. The cold crystallization temperature (T_{cc}) and ΔH_{cc} of the PLA component increase with the addition of BPE, indicating an increase in the degree of cold crystallization of PLA. The incorporation of flexible and branched BPE chains resulted in larger free volume of PLA chains than neat PLA. Consequently, BPE improved the mobility of PLA segment, and thus the cold crystalline ability of PLA was enhanced

Rheological Properties. TPVs can be processed by common plastic processing equipment, such as extruders, injection and molders. Hence a thorough understanding of the flow behavior of biobased TPVs under high shear is important to the determination of processing parameters. To explore the influence of the blending ratio on the rheological properties of biobased TPVs, a strain sweep test was carried out at 180 °C. Figure 5 displays the variations of storage modulus (elastic modulus, G'), loss modulus (viscous modulus, G''), loss factor (tan $\delta = G'/G''$) and complex viscosity (η^*) with strain amplitude for the biobased TPVs. The G' of the biobased TPVs exhibits a linear region at low

strains and nonlinear region at high strains. It can be clearly seen that G' progressively decreases with the increase of strain, similar the so-called Payne effect of filled rubber systems. Thus, the rheological properties of TPVs can be analogically compared with that of the filled rubber system. According to the Payne effect, the nonlinearity of G' is related to the disintegration of the secondary network of filler agglomerates. However, the secondary structure of TPVs corresponds to the crosslinked BPE domains dispersed in the PLA matrix in the form of aggregates and/or agglomerates. We can infer that this nonlinearity of TPVs is associated with the disintegration of agglomerated BPE domains and the debonding of crosslinked BPE domains from the PLA matrix. The G' increases with the increasing BPE content because a higher content of crosslinked BPE results in more elastic biobased TPVs and tend to form the strong networks of crosslinked BPE to PLA.

The strain dependency of G'' of biobased TPVs is presented in Figure 5(b). G'' shows a maximum in the transition region from the linear to nonlinear viscoelastic behavior. Generally, G' is related to the formation of filler networks and G'' to the breakdown and reformation of these structures. The variation of G'' on strain depends on the rates of network breakdown and reformation as well as the sliding of macromolecular chains at the domain surface. The value of loss maximum increases with the increase of BPE content and appears at high strains. Biobased TPVs with higher BPE contents have stronger networks, and the breakdown of larger crosslinked agglomerated BPE domains dissipates more energy. The loss factor is determined by both the loss and the storage modulus (tan $\delta = G'/G''$). It can be seen from Figure 5(c) that biobased TPVs are more elastic ($G' > G''$) in the low strain region. With increasing strain, the G' and G'' curves intersect at tan δ = 1 ($G'=G''$). This

intersection denotes the transition from elastic to viscous behavior. With further increases in strain, the biobased TPVs become more viscous. The high elasticity at high content of crosslinked BPE is manifested by a substantial shift of the intersection point to higher strains.

The complex viscosity (η^*) of biobased TPVs is shown in Figure 5(d). All biobased TPVs exhibit a decrease in η^* with increasing strain, an indication of the shear thinning behavior of polymers. According to the entanglement theory, the decrease in viscosity is attributed to a decrease in the entanglement deformation of the entanglement network. The η^* of biobased TPVs present a much lower rate of decline with strain at low strains than at high strains. The behavior at low strains is related to the strong network and molecular entanglement brought by crosslinked BPE to crosslinked BPE and crosslinked BPE to PLA. As the strain increases, the network tends to collapse and deform, exhibiting higher shear thinning behavior. As shown in Figure 5(a), biobased TPVs with high BPE contents have high viscosity, similarly to the highly filled rubber systems. The shear thinning behavior of biobased TPVs with increasing strain rate is an indication of the good processability of these materials.

Mechanical Properties. The stress-strain curves of the biobased TPVs with various blending ratios are shown in Figure 6, and the relative data are summarized in Table 2. Neat PLA shows very high tensile strength and low elongation at break, characteristic features of a brittle material, while neat BPE shows low tensile strength and high elongation at break, typical elastomeric characteristics. Compared with that of neat PLA, the stress-strain curves of biobased TPVs change from plastic (with necking and yielding) to elastic behavior (without necking and yielding). As shown in Figure 6, the tensile strength and hardness of the biobased TPVs decrease with increasing BPE content,

range from 17.8 MPa to 7.4 MPa and 97º to 86º, respectively, implying the PLA phase is a major factor determining the tensile strength and hardness. The permanent set decreases with increasing BPE content. In addition, the elongation at break at a blending ratio of 80/20 (BPE/PLA, w/w) is relatively low, presumably because of the nonuniform distribution of the crosslinked BPE particles in the PLA matrix (as shown in Figure 3(c)). Generally, TPVs exhibit large reversibility and small residual strains. The elastomeric crosslinked BPE particles dispersed in the PLA matrix make the biobased TPVs recoverable from a highly deformed state. As a result, the higher the BPE contents, the smaller the tensile set at break and the higher the elasticity, as shown in Figure 6(b). The tensile sets at break of the biobased TPVs with a BPE content higher than 70% are smaller than 30%, indicating excellent elastic recovery.

Reprocessability of Biobased TPVs. An advantage of TPVs over conventional thermosetting rubbers is that TPVs can be reprocessed without significantly changing their physical properties. To examine the reprocessability of the biobased TPVs, the tensile properties of the TPV with a blending ratio of 70/30 were measured after the TPV was reprocessed one, three, and five times, and the results are shown in Figure 7. Figure 7 shows that the tensile strength and elongation at break of the TPV do not change significantly after it was reprocessed one and three times. These results indicate that the biobased TPVs can be reprocessed without significant reduction of mechanical properties, behaving like a TPE. However, the tensile strength significantly decreases after the TPV was reprocessed five times because of the breakdown of crosslinked BPE domain from the strain during the process.

To track the changes of rheological properties of the biobased TPVs after reprocessing, we

adopted RPA to simulate the molding cycle. Strain scanning was used to simulate the mixing process and the TPV was kept in the die at 180 °C for 5 min to simulate the molding process. The complex modulus (G^*) and complex viscosity (η^*) as a functional of strain for the biobased TPVs with a blending ratio of 70/30 are shown in Figure 8. The variations of G^* and η^* at low and high strain amplitudes in all the five strain sweeps are shown in Table 3. The G^* and η^* decrease with increasing strain amplitude, manifestations of the Payne effect. Both G^* and η^* slightly decrease with the number of sweep tests at the same strain amplitude. The modulus G^* at a strain of 1% recovers to 90% and 70% of the initial modulus in the 2nd sweep and 5th run sweep, respectively, while the G^* at 470% strain is recovers to only 75% and 49% in the 2nd sweep and 5th run sweep, respectively. The changes of η^* are similar to those of G^*. These results are attributed to the irreversible deformation of the network formed by the disintegration of crosslinked BPE aggregates and debonding of BPE domains from the PLA matrix, as well as the rupture of chain entanglements and chains connecting the aggregates, corresponding to the Mullins effect or stress softening effect. However, the changes of G^* and η^* in the low strain region are readily recovered, suggesting that the BPE domains form highly elastic networks at low strains.

***Biocompatibility*.** The cytotoxicity of a material is evaluated to determine whether it is suitable for biomedical applications. In vitro cytotoxicity testing by MTT colorimetry is used to evaluate the biocompatibility of a material. L929 mouse fibroblasts were used in our cytotoxicity assays by observing the number and morphology of L929 cells in extract. The values of optical density (OD) correspond to the number of the live cells in the extract. Based on the cell relative growth rates (RGR) calculated from the OD values, the cytotoxicity of materials can be classified into six grades,

which are shown in Table 4. Grades 0 and 1 mean that the material presents very low or no cytotoxicity to L929 cells, and grades 0 and 1are accepted as "qualified" in biomedicine. A material with Grade 2 should be further considered by combining with cell morphology. Other grades are regarded as "unqualified," indicating that the material presents very high cytotoxicity and cannot be used as a biomaterial.

The RGR values of the biobased TPVs are displayed in Figure 9. The RGR values of all TPVs are higher than 75%, indicating that all TPVs belong to grade 1 and show low cytotoxicity to L929 cells. These results demonstrate that our biobased TPVs have acceptable biocompatibility. The morphologies of L929 cells incubated for 3 days in the negative control and extract solutions are shown in Figure 10. As shown in Figure 10(a)–(d), the L929 cells show a normal stellate morphology and no negative response, implying that the cells are in good condition. Besides, the cell densities of the biobased TPVs are similar to that of the negative control. In conclusion, our cytotoxicity assays indicated that the biobased TPVs could be potentially used as biomedical materials.

CONCLUSION

In the present work, we have developed novel biobased TPVs via the dynamic crosslinking of biobased polyester elastomer (BPE) and polylactide (PLA), in which a large amount of crosslinked BPE particles were dispersed in PLA matrix. The TEM results showed that the BPE particles had an average diameter of 1 to 4 μm in bioabased TPVs. The glass transition temperatures of BPE and PLA shifted towards each other, indicating some compatibility between BPE and PLA. The rheological studies revealed that the dispersed BPE phase formed an agglomerate network in the

biobased TPVs. The storage modulus and complex viscosity increase with the increasing BPE content, because the elasticity and the viscosity of biobased TPVs increase with increasing degree of crosslinking of BPE. The tensile strength and elongation at break of the biobased TPVs ranged from 11.4 MPa to 17.8 MPa and 154% to 184%, respectively. The tensile sets at break of the biobased TPVs with a BPE content higher than 70% are smaller than 30%, indicating excellent elastic recovery. The biobased TPVs showed no significant decrease in mechanical properties after reprocessing for up to three times. The changes of G^* and η^* in the low strain region after reprocessing are readily recovered, suggesting that the BPE particles formed a strongly elastic network in the low strain region. The cytotoxicity assay indicated that the biobased TPVs showed no cytotoxicity to L929 cells. These biobased TPVs have proved to apply in both biomedical and engineering fields.

ACKNOWLEDGEMENTS. This work was supported by the National Basic Research Program of China (Grant No. 2011CB606003), the National Science & Technology Support Program of China (Grant No. 2013BAE02B02), and the National Natural Science Foundation of China (Grant Nos. 50933001 and 51221002).

REFERENCES

[1] Rader CP. Handbook of thermoplastic elastomers: Van Nostrand Reinhold; 1988.

[2] Spontak RJ, Patel NP. Thermoplastic elastomers: fundamentals and applications. Current Opinion in Colloid & Interface Science 2000;5:333-40.

[3] Abdou-Sabet S, Puydak R, Rader C. Dynamically vulcanized thermoplastic elastomers. Rubber chemistry and technology 1996;69:476-94.

[4] De S, Bhowmick AK. Thermoplastic elastomers from rubber-plastic blends: Ellis Horwood London; 1990.

[5] Karger-Kocsis J. Thermoplastic rubbers via dynamic vulcanization. PLASTICS ENGINEERING-NEW YORK- 1999;52:125-54.

[6] Babu RR, Naskar K. Recent developments on thermoplastic elastomers by dynamic vulcanization. Advanced Rubber Composites: Springer; 2011. p. 219-47.
[7] Coran AY, Patel R. Rubber-thermoplastic compositions. Part I. EPDM-polypropylene thermoplastic vulcanizates. Rubber Chemistry and Technology 1980;53:141-50.
[8] Coran AY, Patel RP, Williams D. Rubber-thermoplastic compositions. Part V. Selecting polymers for thermoplastic vulcanizates. Rubber Chemistry and Technology 1982;55:116-36.
[9] George J, Varughese K, Thomas S. Dynamically vulcanised thermoplastic elastomer blends of polyethylene and nitrile rubber. Polymer 2000;41:1507-17.
[10] Machado A, Van Duin M. Dynamic vulcanisation of EPDM/PE-based thermoplastic vulcanisates studied along the extruder axis. Polymer 2005;46:6575-86.
[11] Oderkerk J, Groeninckx G. Morphology development by reactive compatibilisation and dynamic vulcanisation of nylon6/EPDM blends with a high rubber fraction. Polymer 2002;43:2219-28.
[12] Jha A, Bhowmick AK. Thermoplastic elastomeric blends of nylon-6/acrylate rubber: influence of interaction on mechanical and dynamic mechanical thermal properties. Rubber chemistry and technology 1997;70:798-814.
[13] Van Dyke J, Gnatowski M, Koutsandreas A, Burczyk A. Effect of butyl rubber type on properties of polyamide and butyl rubber blends. Journal of applied polymer science 2004;93:1423-35.
[14] Loercks J. Properties and applications of compostable starch-based plastic material. Polymer Degradation and Stability 1998;59:245-9.
[15] Garlotta D. A literature review of poly (lactic acid). Journal of Polymers and the Environment 2001;9:63-84.
[16] Reddy C, Ghai R, Kalia VC. Polyhydroxyalkanoates: an overview. Bioresource technology 2003;87:137-46.
[17] Simon J, Müller H, Koch R, Müller V. Thermoplastic and biodegradable polymers of cellulose. Polymer degradation and stability 1998;59:107-15.
[18] Swain S, Biswal S, Nanda P, Nayak PL. Biodegradable soy-based plastics: opportunities and challenges. Journal of Polymers and the Environment 2004;12:35-42.
[19] John RP, Nampoothiri KM, Pandey A. Fermentative production of lactic acid from biomass: an overview on process developments and future perspectives. Applied Microbiology and Biotechnology 2007;74:524-34.
[20] Wang Y, Ameer GA, Sheppard BJ, Langer R. A tough biodegradable elastomer. Nature biotechnology 2002;20:602-6.
[21] Bruggeman JP, de Bruin B-J, Bettinger CJ, Langer R. Biodegradable poly (polyol sebacate) polymers. Biomaterials 2008;29:4726-35.
[22] Lei L, Ding T, Shi R, Liu Q, Zhang L, Chen D, et al. Synthesis, characterization and in vitro degradation of a novel degradable poly ((1, 2-propanediol-sebacate)-citrate) bioelastomer. polymer degradation and stability 2007;92:389-96.
[23] Wei T, Lei L, Kang H, Qiao B, Wang Z, Zhang L, et al. Tough Bio‐Based Elastomer Nanocomposites with High Performance for Engineering Applications. Advanced Engineering Materials 2012;14:112-8.
[24] Wang R, Ma J, Zhou X, Wang Z, Kang H, Zhang L, et al. Design and Preparation of a Novel

Cross-Linkable, High Molecular Weight, and Bio-Based Elastomer by Emulsion Polymerization. Macromolecules 2012;45:6830-9.

[25] Wang Z, Zhang X, Wang R, Kang H, Qiao B, Ma J, et al. Synthesis and characterization of novel soybean-oil-based elastomers with favorable processability and tunable properties. Macromolecules 2012;45:9010-9.

[26] Bueno-Ferrer C, Hablot E, Perrin-Sarazin F, Garrigós MC, Jiménez A, Averous L. Structure and Morphology of New Bio-Based Thermoplastic Polyurethanes Obtained From Dimeric Fatty Acids. Macromolecular Materials and Engineering 2012;297:777-84.

[27] Kobayashi T, Matsumura S. Enzymatic synthesis and properties of novel biodegradable and biobased thermoplastic elastomers. Polymer Degradation and Stability 2011;96:2071-9.

[28] Wanamaker CL, O'Leary LE, Lynd NA, Hillmyer MA, Tolman WB. Renewable-Resource Thermoplastic Elastomers Based on Polylactide and Polymenthide. Biomacromolecules 2007;8:3634-40.

[29] Kang H, Qiao B, Wang R, Wang Z, Zhang L, Ma J, et al. Employing a novel bioelastomer to toughen polylactide. Polymer 2013;54:2450-8.

[30] Antunes CF, Machado A, Van Duin M. Morphology development and phase inversion during dynamic vulcanisation of EPDM/PP blends. European Polymer Journal 2011;47:1447-59.

[31] Wu H, Tian M, Zhang L, Tian H, Wu Y, Ning N. New understanding of microstructure formation of the rubber phase in thermoplastic vulcanizates (TPV). Soft matter 2014;10:1816-22.

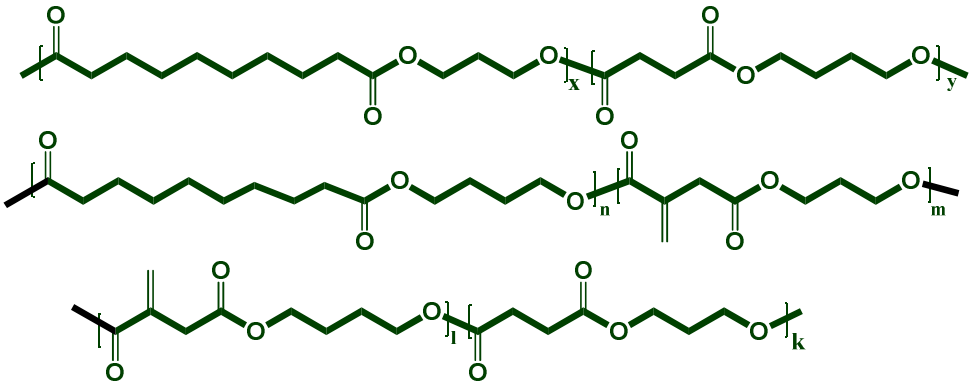

Scheme 1. Chemical structures of Biobased polyester elastomer (BPE).

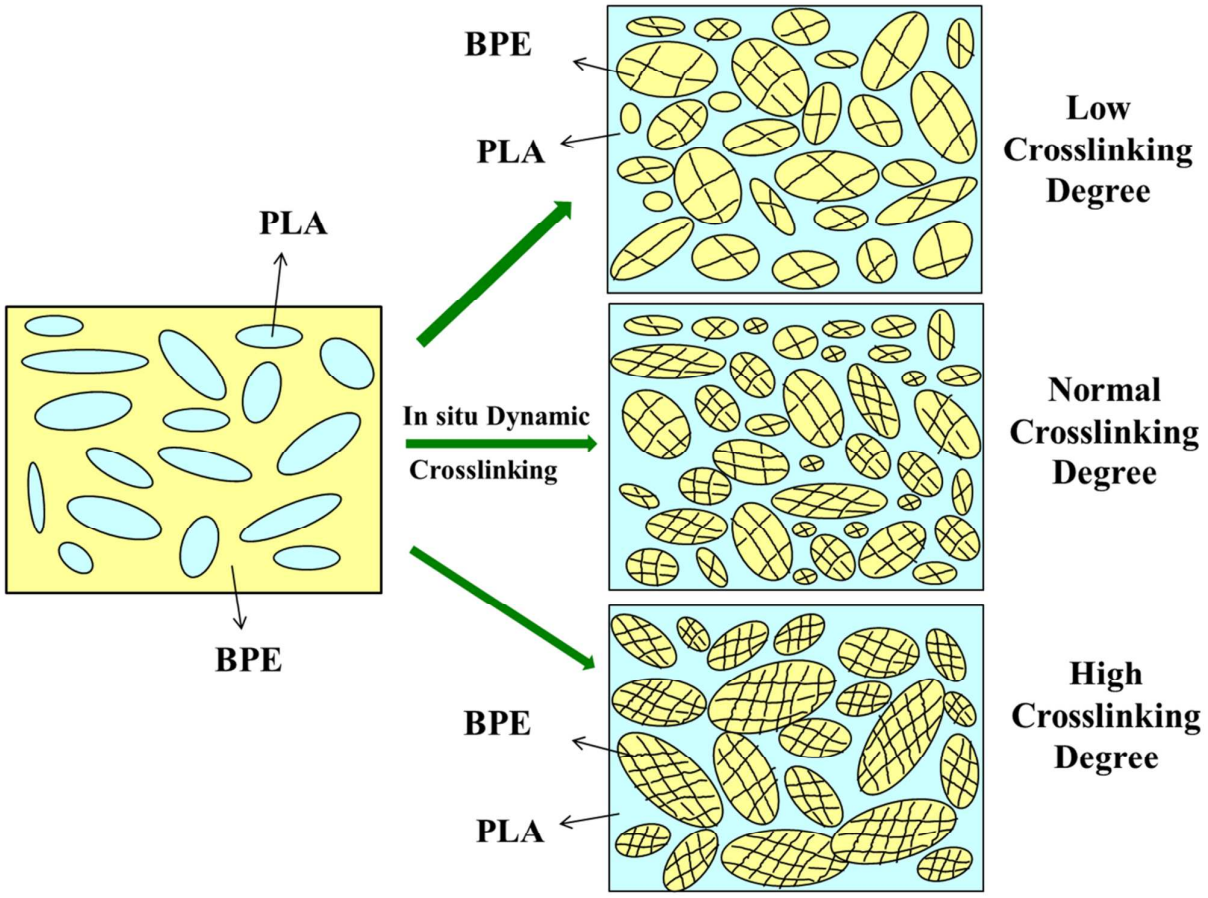

Scheme 2. Phase inversion of biobased TPVs with different degrees of crosslinking.

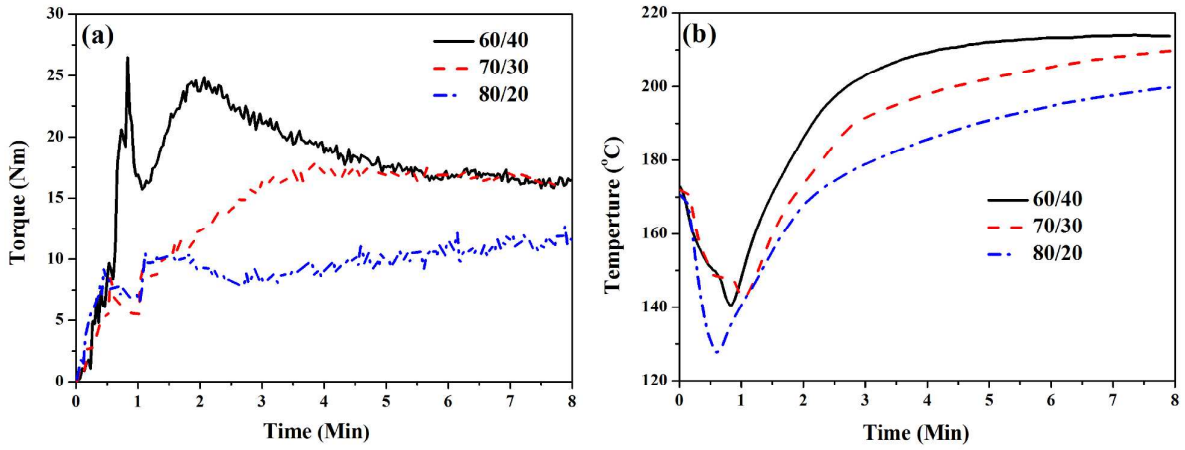

Figure 1. The dynamic vulcanization curves of BPE/PLA blends with different blending ratios of BPE/PLA: (a) mixing torque vs time; (b) mixing temperature vs time.

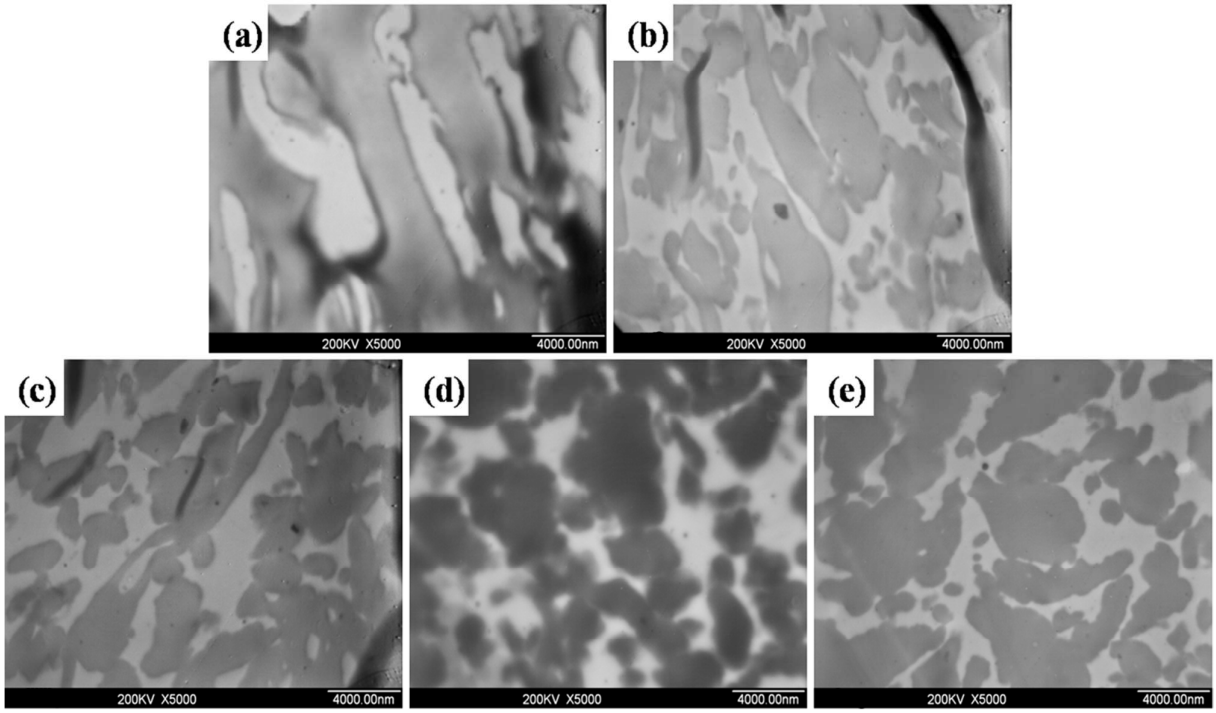

Figure 2. TEM micrographs of biobased TPVs (BPE/PLA,w/w, 70/30) with different DCP contents: (a) 0 phr; (b) 0.02 phr; (c) 0.06 phr; (d) 0.11 phr; (e) 0.22 phr.

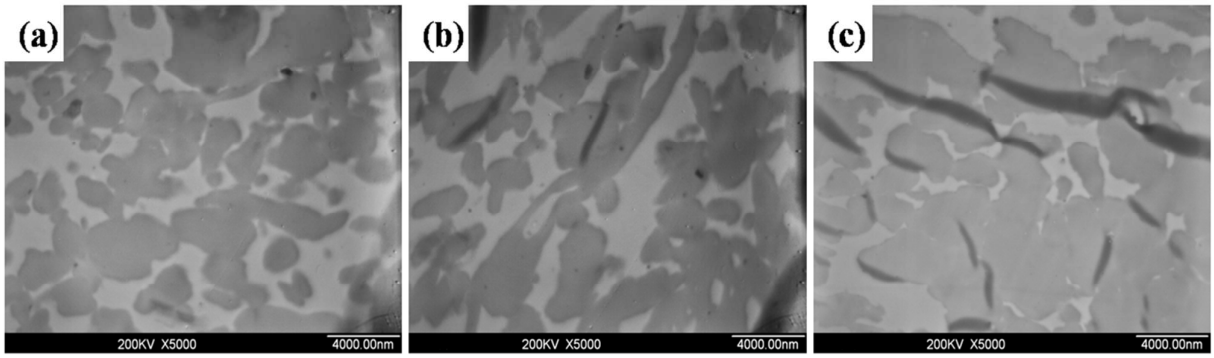

Figure 3. TEM micrographs of biobased TPVs with different blending ratios of BPE/PLA: (a) 60/40; (b) 70/30; (c) 80/20.

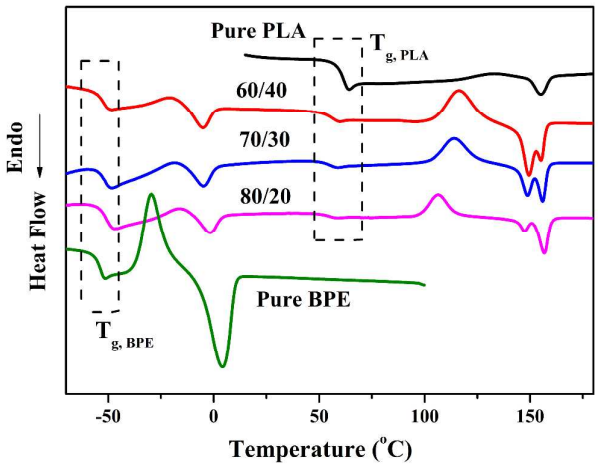

Figure 4. DSC traces of biobased TPVs with different blending ratios of BPE/ PLA.

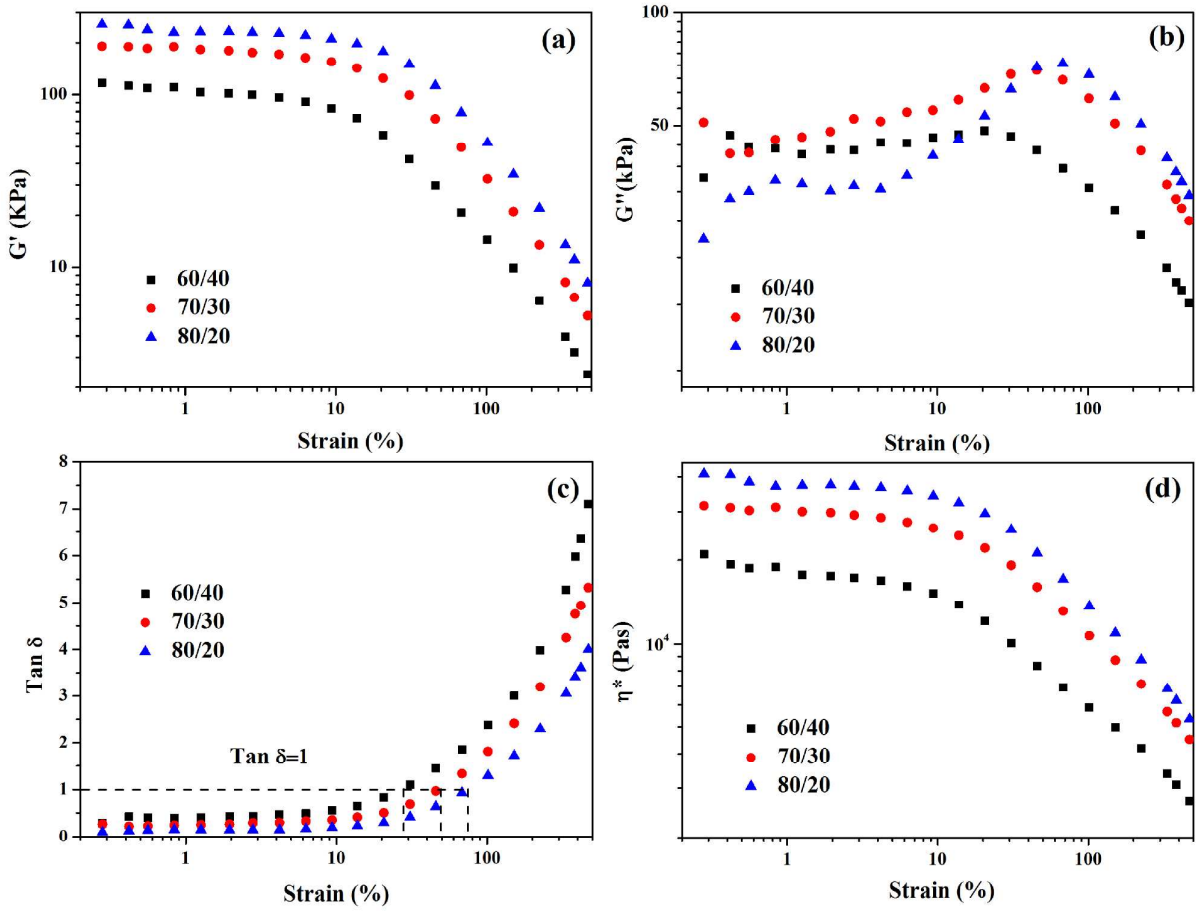

Figure 5. Rheological properties of biobased TPVs with different blending ratios of BPE/PLA at 180 ºC: (a) Storage modulus (G'); (b) Loss modulus (G''); (c) Loss factor (tan δ = G'/G''); (d) Complex viscosity (η^*).

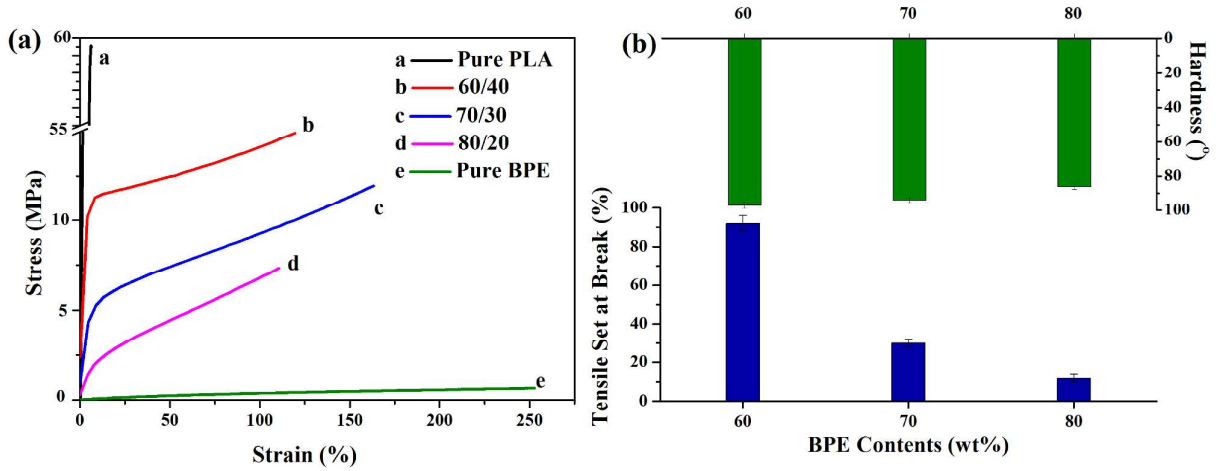

Figure 6. (a) Strain-stress curves of biobased TPVs with different blending ratios of BPE/PLA; (b) Tensile set at break and hardness at different of BPE contents.

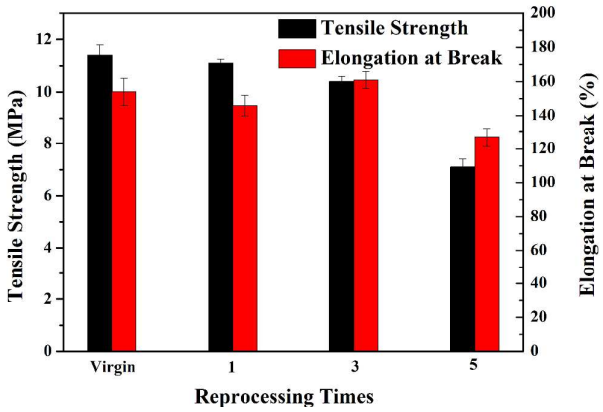

Figure 7. Variations of tensile properties of biobased TPVs (BPE/PLA, 70/30) with number of reprocessing.

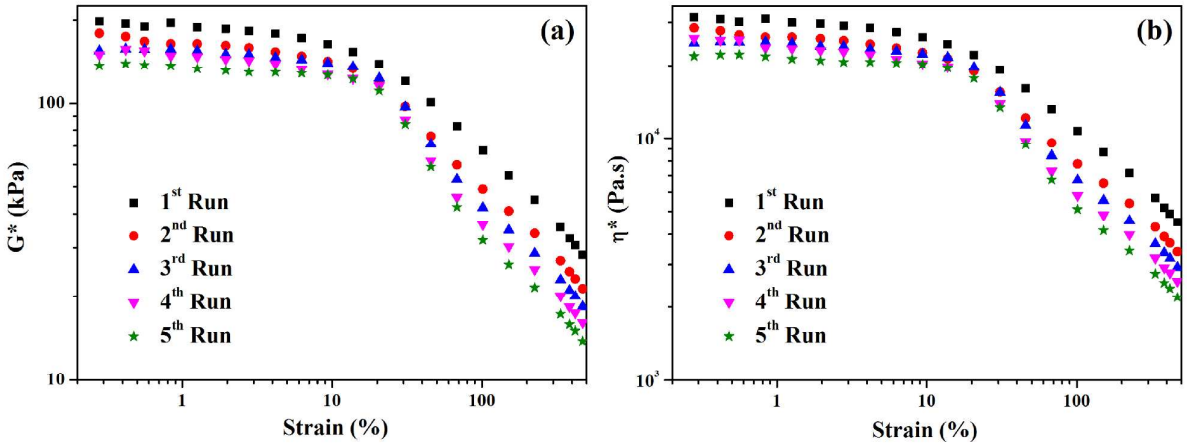

Figure 8. Rheological properties of biobased TPVs (BPE/PLA, 70/30) at 180 ºC after each scanning sweep: (a) Complex modulus (G^*); (b) Complex viscosity (η^*).

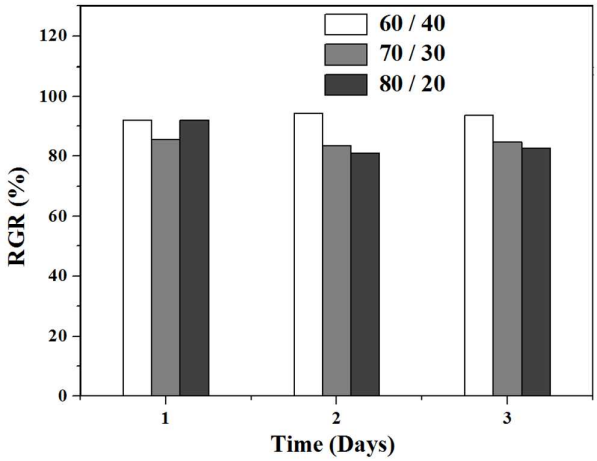

Figure 9. RGR values of biobased TPVs at different incubation time.

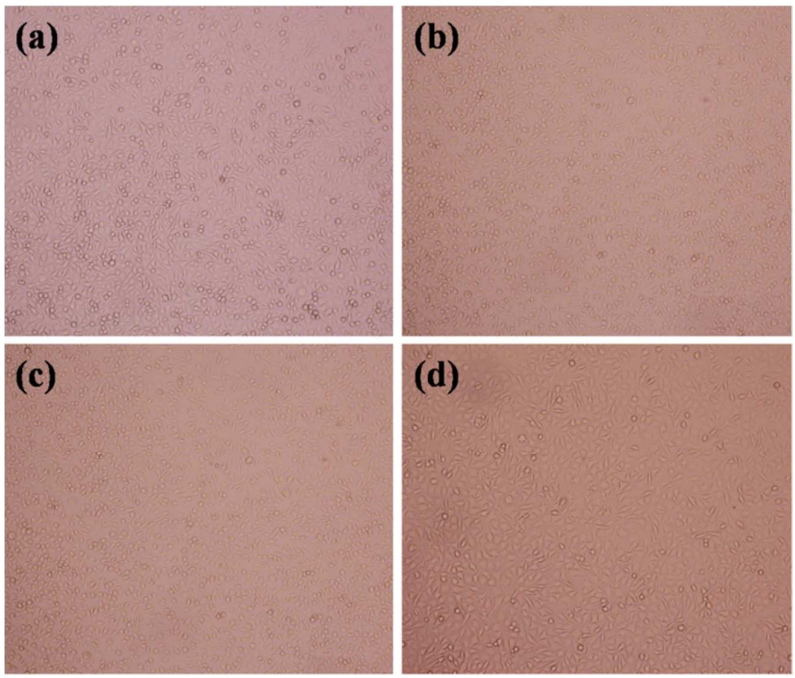

Figure 10. Morphologies of L-929 cells after 3 days' incubation in the negative control and extract solutions of biobased TPVs: (a) 60/40; (b) 70/30; (c) 80/20; (d) the negative control.

Table 1. Thermal properties of biobased TPVs with different blending ratios of BPE/PLA

BPE/PLA	BPE					PLA				
	T_g (°C)	T_{cc} (°C)	ΔH_{cc} (J/g)	T_m (°C)	ΔH_m (J/g)	T_g (°C)	T_{cc} (°C)	ΔH_{cc} (J/g)	T_m (°C)	ΔH_m (J/g)
0/100	-	-	-	-	-	60.0	133.0	2.1	155.1	2.4
60/40	-52.3	-20.3	4.8	-5.0	5.5	54.5	128.7	27.4	155.2	27.5
70/30	-51.5	-19.0	3.0	-4.8	4.2	54.6	113.9	26.1	155.9	27.5
80/20	-51.0	-15.7	3.0	-1.7	3.5	53.7	106.5	25.6	156.6	27.8
100/0	-54.1	-29.5	21.8	4.3	22.6	-	-	-	-	-

The values of ΔH_{cc}, ΔH_m were normalized.

Table 2. Mechanical properties of biobased TPVs with different blending ratios of BPE/PLA

BPE/PLA	Tensile strength （MPa）	Elongation at break（%）	Tensile set at break（%）	Shore A hardness（°）
0/100	54.0±3.8	7±1	-	-
60/40	17.8±1.4	184±15	92±4	97
70/30	11.4±0.4	154±8	30±2	94
80/20	7.4±0.7	120±8	12±2	86
100/0	0.8±0.1	253±7	0	56

Table 3. Rheological data of biobased TPVs (BPE/PLA, 70/30) at 180 ºC by different RPA running.

	First run	Second run	Third run	Fourth run	Fifth run
G^{*a}	195.5	164.3	157.3	148.7	137.1
G^{*b}	28.3	21.3	18.3	16.1	13.8
η^{*c}	31108	26154	25029	23665	21818
η^{*d}	4505	3397	2919	2563	2193

[a] Low strain complex modulus (modulus at 1%; kPa).
[b] High strain complex modulus (modulus at 470%; kPa).
[c] Low strain complex viscosity (viscosity at 1%; kPa).
[d] High strain complex viscosity (viscosity at 470%; kPa).

Table 4. Relationship between cell relative growth rate (RGR) and cytotoxicity grade of a material.

RGR (%)	≥100	75-99	50-74	25-49	1-24	0
Cytotoxicity grade	0	1	2	3	4	5